International Journal of Nanomedicine

Dovepress
open access to scientific and medical research

Open Access Full Text Article

ORIGINAL RESEARCH

A comparative study of toxicity of TiO_2, ZnO, and Ag nanoparticles to human aortic smooth-muscle cells

This article was published in the following Dove Press journal:
International Journal of Nanomedicine

Maolin Wang[1,*]
Qianyu Yang[1,*]
Jimin Long[1]
Yanghuai Ding[1]
Xiaoqing Zou[1]
Guochao Liao[2]
Yi Cao[1]

[1]Key Laboratory of Environment-Friendly Chemistry and Application of Ministry of Education, Laboratory of Biochemistry, College of Chemistry, Xiangtan University, Xiangtan, Hunan 411105, People's Republic of China; [2]International Institute for Translational Chinese Medicine, Guangzhou University of Chinese Medicine, Guangzhou, Guangdong 510006, People's Republic of China

*These authors contributed equally to this work

Purpose: To evaluate the adverse vascular effects of nanoparticles (NPs) in vitro, extensive studies have investigated the toxicity of NPs on endothelial cells, but the knowledge of potential toxicity on human smooth-muscle cells (SMCs) is currently limited.

Methods: This study compared the toxicity of TiO_2, ZnO, and Ag NPs to human aortic SMCs.

Results: Only ZnO NPs significantly induced cytotoxicity, accompanied by increased intracellular reactive oxygen species, Zn ions, and endoplasmic reticulum stress biomarkers (*DDIT3* expression and p-Chop proteins). All the NPs significantly promoted the release of soluble VCAM1 and soluble sICAM1, but not IL6, which suggested that metal-based NPs might promote inflammatory responses. Furthermore, *KLF4* expression (a transcription factor for SMC-phenotype switch) was significantly induced by TiO_2 NPs and modestly by ZnO NPs, but the expression of *CD68* remained unaltered.

Conclusion: Our data indicated that ZnO NPs were more cytotoxic to human aortic SMCs than TiO_2 and Ag NPs at the same mass concentrations, which might have been associated with intracellular reactive oxygen species, Zn ions, and endoplasmic reticulum stress.

Keywords: metal-based nanoparticles, NPs, human aortic smooth-muscle cells, HASMCs, cytotoxicity, inflammation, endoplasmic reticulum stress, ER stress

Introduction

At present, metal-based nanoparticles (NPs), particularly TiO_2, ZnO, and Ag NPs, are among the most produced and used NPs, and have already been used in many commercially available products, such as health care products, food-related products, and electronics.[1] Therefore, it is necessary and urgent to assess the potential toxicity and mechanisms of metal-based NP exposure, both in vivo and in vitro. Recently, the potential adverse effects of NPs to cells lining blood vessels have gained extensive research interest, because the contact of human blood vessels with metal-based NPs could be increased for two main reasons. First, due to their smallness, metal-based NPs are able to pass the physiological barriers and translocate into the bloodstream. Indeed, this possibility has been proven by extensive studies showing the systemic distribution of metal-based NPs in animals after oral and inhalational exposure.[2] Second, the use of metal-based NPs in biomedicine could lead to direct contact of human blood vessels with these NPs, which suggests that it is necessary to evaluate the toxicity of metal-based NPs to cells lining blood vessels.[3,4]

Extensive studies have already evaluated the toxicity of metal-based NPs to human endothelial cells, the surface cells covering the lumen of blood vessels.[2] However, the toxicity of NPs to smooth-muscle cells (SMCs) has gained less attention. SMCs play

Correspondence: Guochao Liao
International Institute for Translational Chinese Medicine, Guangzhou University of Chinese Medicine, Waihuan East Road No 232, Guangzhou, Guangdong 510006, People's Republic of China
Tel +86 20 3935 8843
Email liao@gzucm.edu.cn

Yi Cao
Key Laboratory of Environment-Friendly Chemistry and Application of Ministry of Education, Laboratory of Biochemistry, College of Chemistry, Xiangtan University, Erhuan North Road No 15, Xiangtan, Hunan 411105, People's Republic of China
Tel +86 731 5829 2251
Email caoyi39@xtu.edu.cn

submit your manuscript | www.dovepress.com
Dovepress
http://dx.doi.org/10.2147/IJN.S188175

an important role in the regulation of blood-vessel function, as they are key determinants of arterial wall remodeling, cell–extracellular matrix interactions, and inflammatory responses.[5] In addition, SMCs might undergo phenotype switch, which could directly promote atherosclerosis.[6] Despite the importance of SMCs in the maintenance of blood-vessel function, relatively few studies have evaluated the toxicity of NPs to SMCs. Indeed, to the best of our knowledge, only one study has shown that intravenous and gastric CeO_2 NP exposure impaired SMC signaling in rats.[7] There is currently a lack of in vitro study to link the adverse effects of NP exposure directly to SMCs.[8]

The present study compared the toxicity of TiO_2, ZnO, and Ag NPs to human aortic SMCs (HASMCs) in vitro. To link the physicochemical properties of metal-based NPs to the toxic effects to HASMCs, the present study thoroughly characterized all the NPs by multiple techniques, ie, transmission electron microscopy (TEM), atomic-force microscopy (AFM), and X-ray diffraction (XRD). To investigate the toxic effects of NPs on HASMCs, the cytotoxicity of these NPs was investigated by cell counting kit-8 (CCK8) and neutral red uptake assays, ultrastructural changes were observed by TEM, and release of IL6, soluble vascular cell adhesion molecule 1 (sVCAM1), and soluble intercellular adhesion molecule 1 (sICAM1) determined by ELISA to indicate inflammatory responses. Because the results showed that only ZnO NPs significantly induced cytotoxicity, we further addressed the possible mechanisms associated with the cytotoxicity. To this end, intracellular reactive oxygen species (ROS) and Zn ions were determined, as they have been suggested to be related to the toxicity of ZnO NPs.[9] In addition, the expression of endoplasmic reticulum (ER) stress genes, namely *DDIT3*, *XBP1S*, *ERN1*, and *ATF6* was measured by real-time reverse transcription (RT) PCR, and protein levels of Chop and p-Chop were determined by Western blot. The biomarkers associated with ER stress were measured because recent studies suggested that NP exposure might induce toxicity through the modulation of ER stress.[10] Finally, the expression of *KLF4* and *CD68* molecules was also determined, because they are crucial for SMC-phenotype switch.[5,11]

Methods

Cell culture

HASMCs at passage 1 and related cell-culture reagents were purchased from ScienCell Research Laboratories (Carlsbad, CA, USA). HASMCs were initially expanded in 2 μg/cm^2 poly-D-lysine (PDL)-precoated T75 tissue-culture flasks at a density of >5,000 cells/cm^2. Cells were cultured in SMC medium supplemented with 2% (v:v) FBS, 1% (v:v) SMC growth supplement, and 1% (v:v) penicillin–streptomycin solution in a CO_2 incubator at 37°C for about 7–10 days, with medium changed every 2–3 days. The expanded cells were then harvested by trypsin, collected in cryovials with cell-freezing medium, and preserved in liquid nitrogen at passage 2. The frozen cells were thawed and then cultured in PDL-precoated T25 tissue-culture flasks. During the experimental period, cells were used at passages 3–5.

NP characterization and preparation

The TiO_2 (XFI02, 15–25 nm), ZnO (XFI06, 20 nm), and Ag NPs (XFJ14, 60–80 nm) were purchased from Nanjing XFNano Materials Tech (Nanjing, People's Republic of China). To characterize these NPs, morphology was investigated by TEM (FEI Tecnai G20) accelerated at 200 kV. NP topography was investigated by AFM on a Bruker MultiMode 8 by using PeakForce mode at room temperature. Topographic images were analyzed with NanoScope Analysis 1.8, and AFM heights (mean ± SD) calculated based on measurement of 30 randomly selected NPs. Phase compositions were analyzed with XRD on a Bruker D8 Advanced, and Brunauer–Emmett–Teller surface area was measured using a TriStar II 3020 (Micromeritics, Norcross, GA, USA).

To make the NP suspensions, a stock solution of 1,280 μg/mL particles (prepared in 2% FCS) was continuously sonicated twice for 8 minutes each time with cooling on ice using an ultrasonic processor (FS-250N, 20% amplitude; Shengxi, Shanghai, People's Republic of China). After sonication, suspensions were immediately diluted in cell-culture medium to desired concentrations for exposure, and control cells were incubated with equal amounts of vehicle. To characterize the NPs in suspensions, hydrodynamic size, ζ-potential, and polydispersity index were measured. Here the NPs were diluted as 64 μg/mL in water or cell-culture medium and then analyzed with a Zetasizer Nano ZS90 (Malvern Instruments, Malvern, UK). Data are expressed as mean ± SD of three measurements based on a single run.

Cytotoxicity assays

Cytotoxicity was estimated by CCK8 and neutral red uptake assays, which indicate the activity of mitochondria and lysosomes, respectively. For the assays, HASMCs were seeded at a density of 4×10^4 per well in 24-well plates. After being grown for 2 days, the cells were incubated with 0 μg/mL (control), 4 μg/mL, 8 μg/mL, 16 μg/mL, 32 μg/mL, and 64 μg/mL NPs. After 24-hour exposure, cells were rinsed once and CCK8 and neutral red uptake assays performed

on adherent cells using commercial kits purchased from the Beyotime Institute of Biotechnology (Haimen, People's Republic of China) according to the manufacturer's instructions. The final products were read using ELISA (Synergy HT; BioTek, Winooski, VT, USA). To measure the cytotoxicity of Zn ions, HASMCs grown on 24-well plates were also exposed to 50–800 μM $ZnSO_4$ for 24 hours and a CCK8 assay done.

Ultrastructural observations by TEM

TEM was used to visualize the ultrastructural changes of cells. HASMCs were seeded at a density of 4×10^5 on 60 mm diameter cell-culture petri dishes and grown for 2 days before exposure to 0 μg/mL (control) and 16 μg/mL NPs. After 24-hour exposure, cells were rinsed and removed from the cell-culture dishes using cell scrapers. TEM study was then done as previously described.[12]

Intracellular ROS

Intracellular ROS was measured using a fluorescent probe (dichlorodihydrofluorescein diacetate [DCFH-DA]; Sigma-Aldrich Co., St Louis, MO, USA), which is a general method to assess NP-induced oxidative stress. The assay was done as previously described.[13] Briefly, HASMCs were seeded at a density of 10^4 per well in 96-well black plates. After being grown for 2 days, cells were incubated with 0 μg/mL (control), 4 μg/mL, 8 μg/mL, 16 μg/mL, 32 μg/mL, and 64 μg/mL NPs. After 3-hour exposure, cells were rinsed and intracellular ROS inside adherent cells measured using DCFH-DA. Fluorescent products were read at excitation 485±20 nm and emission 528±20 nm by an ELISA reader.

Intracellular Zn ions

The accumulation of intracellular Zn ions was measured by using a fluorescent probe zinquin ethyl ester (Sigma-Aldrich Co.). Briefly, HASMCs were seeded in black 96-well plates and exposed to various concentrations of NPs. After 3-hour exposure, intracellular Zn ions inside adherent cells were determined by zinquin ethyl ester as previously described.[14]

ELISA

The release of cytokines into cell-culture medium was measured to assess inflammatory responses. Before CCK8 or neutral red uptake assays, supernatants from NP-exposed cells (concentrations 0 μg/mL, 4 μg/mL, 16 μg/mL, and 64 μg/mL) were collected and concentrations of IL6, sVCAM1, and sICAM1 determined using ELISA kits following the manufacturer's instructions (Neobioscience, Guangzhou, People's Republic of China).

Real-time RT-PCR

mRNA levels of *DDIT3*, *XBP1S*, *ERN1*, *ATF6* (ER-stress genes), *KLF4*, *CD68* (SMC phenotype-switch biomarkers), and *GAPDH* (internal control) were determined by quantitative real-time RT-PCR. Briefly, 2×10^5 HASMCs per well were seeded on six-well plates and grown for 2 days before exposure to 0 μg/mL (control) and 64 μg/mL TiO_2, ZnO, or Ag NPs for 3 hours. After exposure, total mRNA in adherent cells was extracted using TRI reagent (Sigma-Aldrich Co., USA). cDNA was synthesized using a HiFiScript kit (CWBiotech, Beijing, People's Republic of China) and quantitative real-time RT-PCR done using an Ultra SYBR mixture (CWBiotech) on a PikoReal quantitative PCR system (Thermo Fisher Scientific, Waltham, MA, USA) following manufacturers' instructions.[12] Primers for each gene are summarized in Table S1. mRNA levels are expressed as the ratio between the mRNA level of the target genes and the internal control gene.

Western blot

Protein level of ER-stress biomarkers, namely Chop and p-Chop, were determined by Western blot. The protein level of β-actin served as the internal control. Briefly, 2×10^5 HASMCs per well were seeded on six-well plates and grown for 2 days before exposure to 0 μg/mL (control) and 64 μg/mL TiO_2, ZnO, or Ag NPs for 3 hours. After exposure, cells were rinsed twice with HBSS and total proteins in adherent cells extracted by RIPA lysis buffer in the presence of a protease-inhibitor cocktail and PhosStop phosphatase inhibitor (Roche Diagnostics). After being on ice for 10 minutes, the supernatants were collected by 15-minute centrifuge at 12,000 rpm, 4°C. Protein concentrations were measured by bicinchoninic acid assay, and 50 μg/sample proteins were mixed with loading buffer and then resolved on SDS-PAGE. Samples were transferred to a nitrocellulose membrane, blocked in nonfat milk for 1.5 hours at room temperature, and then incubated overnight at 4°C with the primary antibody (1:500 p-Chop rabbit antibody, Abcam, Cambridge, UK; 1:800 Chop rabbit antibody, Proteintech, Chicago, IL, USA; 1:5,000 β-actin antibody, Proteintech). Blots were washed in 0.1% w:v Tween-PBS and then incubated with 1:5,000 HRP goat antirabbit IgG (Proteintech) for 1.5 hours. After that, blots were detected with Super ECL Plus chemiluminescence (Thermo Fisher Scientific).

Statistics

Data are expressed as mean ± SD of mean values of three independent experiments. Two-way ANOVA was followed

by Tukey's honest significant difference test using R 3.3.3. $P<0.05$ was considered statistically significant.

Results

Characterization of NPs

TEM (Figure S1) indicated the presence of spherical and irregular particles in all samples. XRD patterns of these NPs (Figure S2) revealed anatase, face-centered cubic, and hexagonal structures for TiO_2, ZnO, and Ag NPs, respectively. AFM (Figure S3) showed uniform and smooth surfaces for all NPs. Physicochemical properties of NPs are summarized in Table 1. AFM heights were in the order Ag > ZnO > TiO_2. Brunauer–Emmett–Teller surface areas were in the order TiO_2 > ZnO > Ag. The hydrodynamic sizes were in the order TiO_2 > ZnO > Ag. It should be noted that average hydrodynamic sizes of TiO_2 and ZnO NPs were much larger than their primary sizes, which suggested that these NPs might easily form agglomerates and/or aggregates in suspensions. All NPs were negatively charged in both water and cell-culture medium. ZnO NPs exhibited a much higher absolute ζ-potential value when they were suspended in water, but the average ζ-potential values of TiO_2, ZnO, and Ag NPs were similar when they were suspended in medium.

Cytotoxicity of NPs

Exposure to up to 64 μg/mL TiO_2 or Ag NPs did not significantly induce cytotoxicity in HASMCs ($P>0.05$), whereas exposure to 32 μg/mL and 64 μg/mL ZnO NPs was associated with significant cytotoxicity on both CCK8 ($P<0.01$; Figure 1) and neutral red uptake assays ($P<0.01$; Figure 1). Light microscopy (Figure S4) indicated that after exposure to 64 μg/mL ZnO NPs, most cells detached from the cell-culture surface, whereas the remaining cells became round without neutral red staining. This effect was not observed in TiO_2- or Ag NP-exposed cells.

Ultrastructural changes and internalization of NPs

TEM images (Figure 2) clearly showed internalization of TiO_2 NPs as agglomerates/aggregates in cytoplasm of HASMCs, but internalization of ZnO and Ag NPs into HASMCs was not obvious. In addition, ZnO NPs appeared to induce intracellular vacuolation of HASMCs more obviously.

Release of inflammatory cytokines

Release of IL6, sVCAM1, and sICAM1 was determined by ELISA to assess inflammatory responses. As shown in Figure 3, exposure to TiO_2, ZnO, and Ag NPs significantly increased release of sVCAM1 and sICAM1, but not IL6. Significantly increased sVCAM1 release was observed following exposure to 4 μg/mL TiO_2 NPs ($P<0.05$), 16 μg/mL ($P<0.01$), and 32 μg/mL ZnO NPs and 4 μg/mL Ag NPs ($P<0.01$). Also, significantly increased sICAM1 release was observed after exposure to 4 μg/mL TiO_2 NPs ($P<0.01$), 16 μg/mL ZnO NPs, ($P<0.05$) and 32 μg/mL Ag NPs ($P<0.05$).

Intracellular ROS and Zn ions

Dose-dependent increases in intracellular ROS were observed only after exposure to ZnO NPs ($P<0.01$), but not TiO_2 or Ag NPs ($P>0.05$; Figure 4). Intracellular ROS were significantly induced following exposure to 32 μg/mL and 64 μg/mL ZnO NPs ($P<0.01$). For intracellular Zn ions (Figure 4), exposure to 8 μg/mL, 16 μg/mL, 32 μg/mL, and 64 μg/mL ZnO NPs significantly promoted intracellular Zn ions in HASMCs ($P<0.01$). Moreover, exposure to 400 μM and 800 μM $ZnSO_4$ significantly induced cytotoxicity to HASMCs (Figure S5; $P<0.01$).

ER stress

The expression of ER-stress genes was determined by real-time RT-PCR. Expression of *DDIT3* (Figure 5) was

Table 1 A summary of physicochemical properties of NPs determined in this study

	BET area (m^2/g)	AFM height (nm)	Hydrodynamic size (nm)	Z-potential (mV)	PDI
TiO_2 (code XFI02)	89.01	21.03±5.33	376.30±13.37 (water); 398.55±1.63 (medium)	−2.37±0.41 (water); −8.9±0.08 (medium)	0.292±0.076 (water); 0.2605±0.013 (medium)
ZnO (code XFI06)	17.60	51.76±10.05	253.83±3.73 (water); 241.15±1.77 (medium)	−22.13±1.05 (water); −6.30±0.25 (medium)	0.121±0.014 (water); 0.415±0.059 (medium)
Ag (code XFJ14)	4.35	94.03±10.02	118.47±8.09 (water); 120.45±15.06 (medium)	−8.03±1.27 (water); −6.51±0.17 (medium)	0.380±0.086 (water); 0.497±0.076 (medium)

Abbreviations: AFM, atomic force microscopy; BET, Brunauer–Emmett–Teller; NPs, nanoparticles; PDI, polydispersity index.

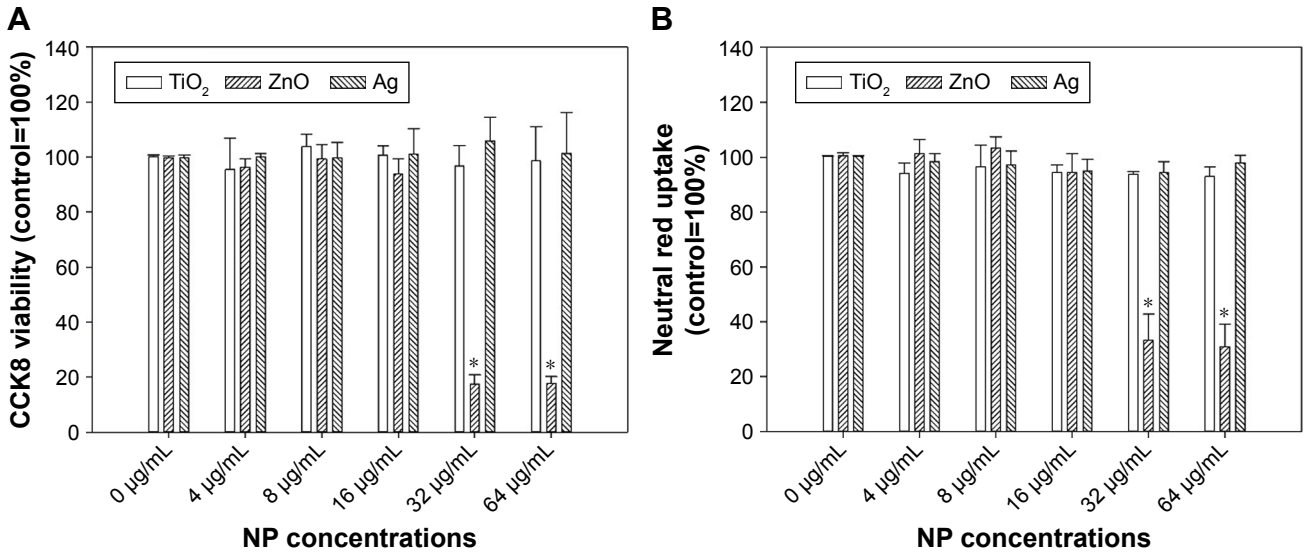

Figure 1 Cytotoxicity of TiO_2, ZnO, and Ag NPs.
Notes: HASMCs were exposed to various concentrations of TiO_2, ZnO, and Ag NPs for 24 hours, and cytotoxicity was assessed by CCK8 (**A**) and neutral red uptake assays (**B**). *$P<0.05$ compared to control.
Abbreviations: CCK8, cell counting kit-8; NPs, nanoparticles; HASMCs, human aortic smooth-muscle cells.

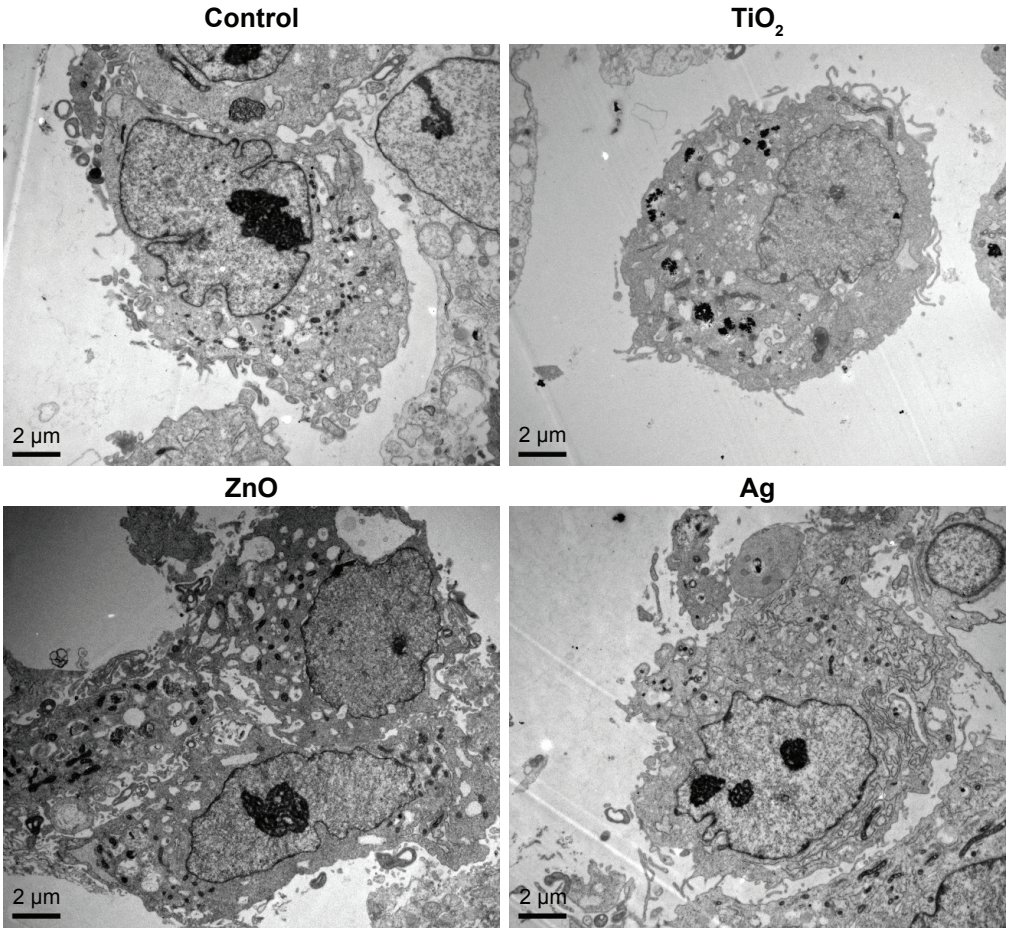

Figure 2 Representative TEM images of HASMCs.
Note: HASMCs were exposed to 0 μg/mL (control), 16 μg/mL TiO_2 NPs, 16 μg/mL ZnO NPs, or 16 μg/mL Ag NPs for 24 hours, and TEM was used to visualize ultrastructural changes in cells and internalization of NPs.
Abbreviations: HASMCs, human aortic smooth-muscle cells; NPs, nanoparticles; TEM, transmission electron microscopy.

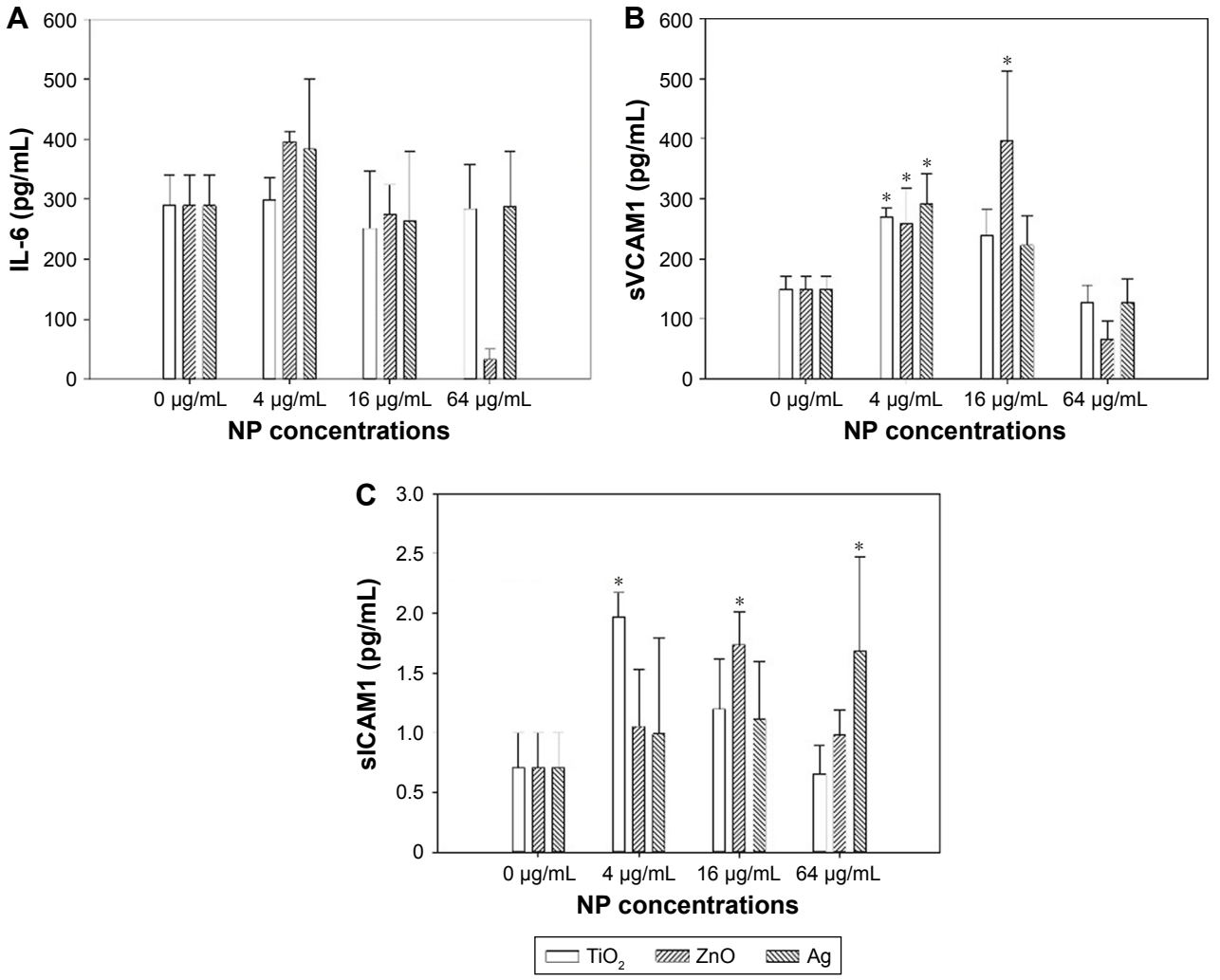

Figure 3 Release of inflammatory cytokines.

Notes: HASMCs were exposed to various concentrations of TiO_2, ZnO, and Ag NPs for 24 hours. Supernatants were collected, and concentrations of IL6 (**A**), sVCAM1 (**B**), and sICAM1 (**C**) were analyzed by ELISA. *$P<0.05$ compared to control.

Abbreviations: HASMCs, human aortic smooth-muscle cells; NPs, nanoparticles sICAM1, soluble intercellular adhesion molecule 1;VCAM1, soluble vascular cell adhesion molecule 1.

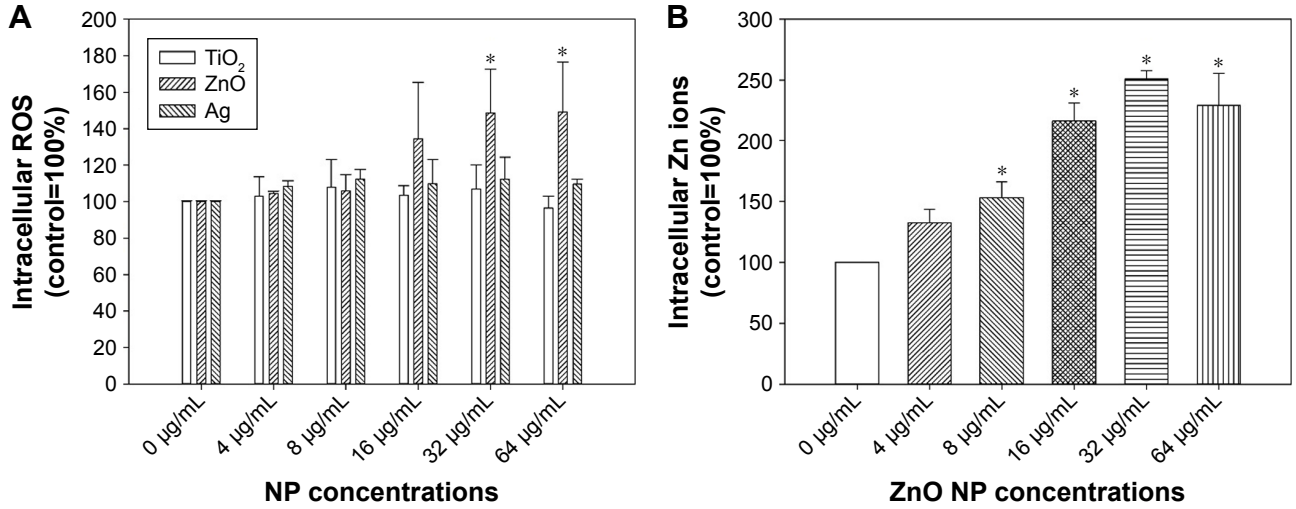

Figure 4 Intracellular ROS (**A**) and Zn ions (**B**).

Notes: (**A**) HASMCs were exposed to various concentrations of TiO_2, ZnO, and Ag NPs for 3 hours and intracellular ROS were determined using a fluorescent probe. (**B**) HASMCs were exposed to various concentrations of ZnO NPs for 3 hours, and intracellular Zn ions were determined using a fluorescent probe. *$P<0.05$ compared to control.

Abbreviations: HASMCs, human aortic smooth-muscle cells; NPs, nanoparticles; ROS, reactive oxygen species.

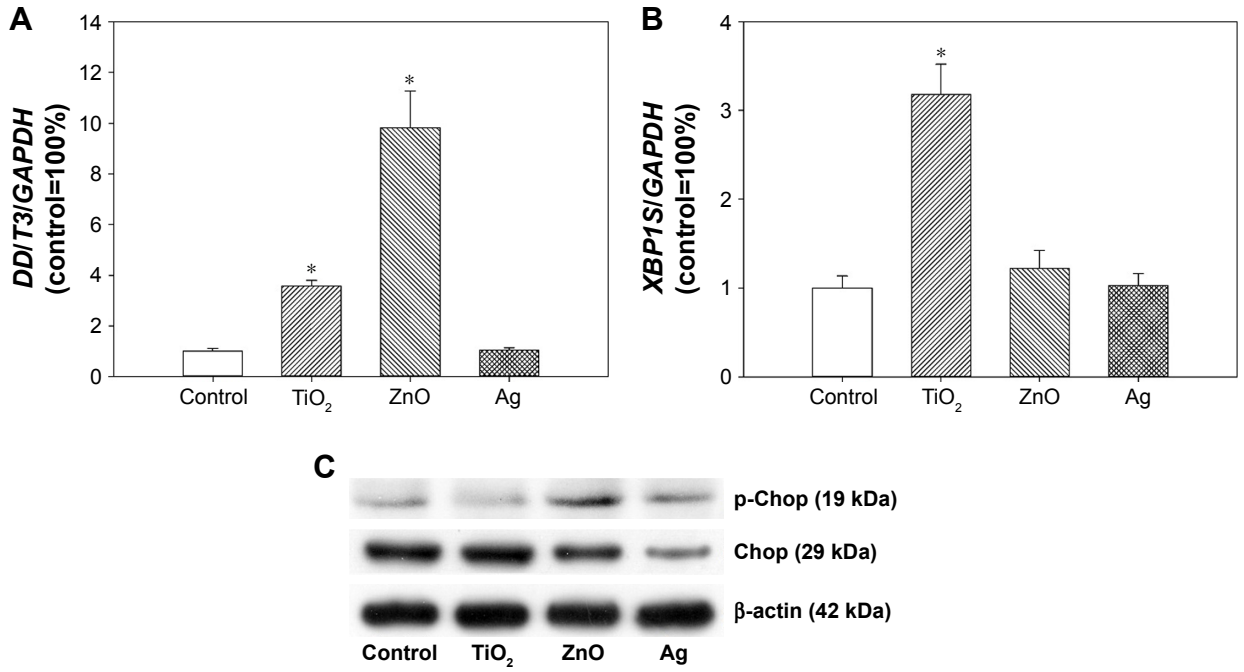

Figure 5 Changes in ER-stress markers.
Notes: HASMCs were exposed to 0 μg/mL (control) and 64 μg/mL TiO_2, ZnO, or Ag NPs for 3 hours, and real-time reverse transcription PCR was used to determine the expression of *DDIT3* (**A**) and *XBP1S* (**B**). mRNA levels of *ERN1* and *ATF6* were not significantly induced by NP exposure (data not shown). *$P<0.05$ compared to control. (**C**) Protein levels of Chop, p-Chop, and β-actin (internal control) determined by Western blot. Unedited Western blot images are shown in Figure S6.
Abbreviations: ER, endoplasmic reticulum; HASMCs, human aortic smooth-muscle cells; NPs, nanoparticles.

significantly induced after exposure to ZnO NPs ($P<0.01$), as well as TiO_2 NPs to a lesser extent ($P<0.05$). For *XBP1S* (Figure 5), significantly increased expression was observed only in cells exposed to TiO_2 NPs ($P<0.01$), but not ZnO or Ag NPs ($P>0.05$). No significant increase in *ERN1* or *ATF6* was observed after NP exposure (data not shown).

Results from Western blot showed that exposure to ZnO NPs and to a lesser extent Ag NPs promoted the protein level of p-Chop. However, the protein level of Chop was not obviously increased after TiO_2 NP exposure (Figure 5).

Expression of *KLF4* and *CD68*

KLF4 expression was significantly induced following exposure to TiO_2 NPs ($P<0.01$), but the difference between control and ZnO NP exposed cells was only marginally significantly different ($P=0.077$). Exposure to metal-based NPs did not significantly affect *CD68* expression ($P>0.05$; Figure 6).

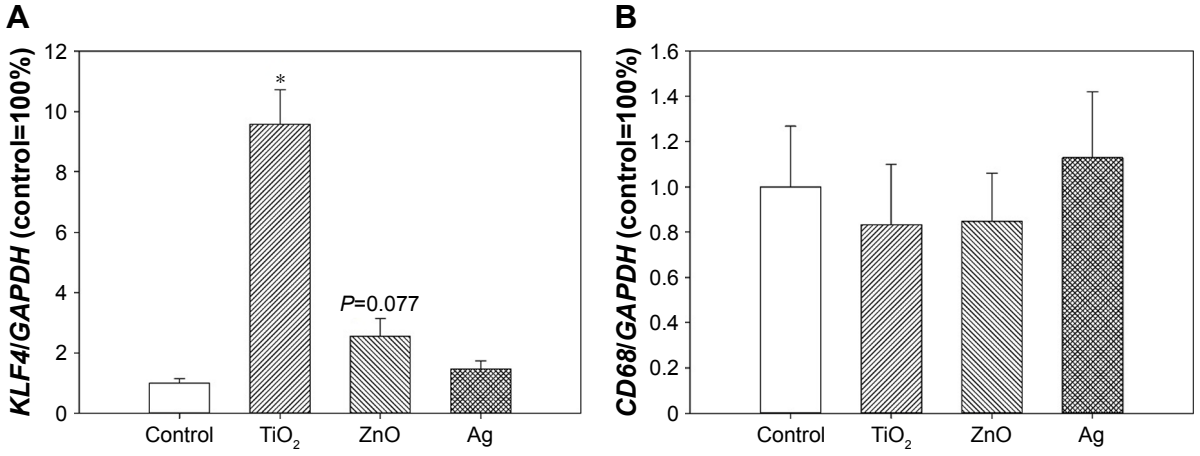

Figure 6 Expression of *KLF4* and *CD68*.
Notes: HASMCs were exposed to 0 μg/mL (control) and 64 μg/mL TiO_2, ZnO, or Ag NPs for 3 hours, and real-time reverse transcription PCR was used to determine the expression of *KLF4* (**A**) and *CD68* (**B**). *$P<0.01$ compared to control.
Abbreviations: HASMCs, human aortic smooth-muscle cells; NPs, nanoparticles.

Discussion

Given the importance of SMCs in the pathophysiology of vascular diseases,[5,6] this study investigated the toxicity of TiO_2, ZnO, and Ag NPs to HASMCs to understand the potential adverse vascular effects of these NPs on blood vessels. It was shown that only ZnO NPs significantly induced cytotoxicity in HASMCs, associated with an increase in intracellular ROS and Zn ions. In addition, exposure to ZnO NPs was also associated with increased mRNA level of *DDIT3* and protein level of p-Chop, which suggested the activation of ER stress. All NPs significantly promoted the release of sVCAM1 and sICAM1, which are biomarkers for inflammatory responses. Moreover, exposure to TiO_2 NPs, as well as ZnO NPs to lesser extent, promoted the expression of SMC-phenotype-switch factor *KLF4*, albeit *CD68* expression was not significantly affected. These results combined indicated that direct contact with metal-based NPs could be toxic to HASMCs.

The cytotoxicity of TiO_2, ZnO, and Ag NPs to HASMCs was investigated by CCK8 and neutral red uptake assays, which reflect damage to mitochondria and lysosomes, respectively. The results showed that up to 64 μg/mL ZnO NPs, but not TiO_2 or Ag NPs at the same mass concentrations, significantly induced cytotoxicity to HASMCs. Similar observations have been reported before by using human endothelial cells.[2,15–17] Moreover, TEM further showed that ZnO NPs more obviously induced intracellular vacuolation of HASMCs. In our recent studies, we also found that NP exposure could induce ultrastructural changes in cells, even though the cytotoxicity of NPs was only modest.[12,18,19] TEM confirmed that ZnO NPs were more cytotoxic than TiO_2 and Ag NPs at the same mass concentrations. It should be noted that using TEM, we observed internalization of only TiO_2 NPs as agglomerates/aggregates inside HASMCs. This could have been due to relatively low concentrations of NPs used in TEM and ZnO and Ag NPs being partially soluble, leading to lowered NP concentrations once internalized.[9,20]

We then tried to address the possible mechanisms of ZnO NP cytotoxicity. It has been suggested that increased intracellular ROS and/or Zn ions play a crucial role in the toxicity of ZnO NPs.[9] Here, we also observed significantly increased intracellular ROS and Zn ions in HASMCs after exposure to ZnO NPs. Moreover, direct contact with $ZnSO_4$ was also cytotoxic to HASMCs, which further confirmed that excessive Zn ions could be cytotoxic. Previous studies have obtained similar conclusions using human endothelial cells that ZnO NPs induced cytotoxicity through the induction of intracellular ROS and Zn ions.[17,21–23] Furthermore, we also investigated activation of the ER-stress pathway, which is an adaptive response to the dysfunction of ER that can result in cell death.[24] The results showed that ZnO NPs promoted the proapoptotic factor *DDIT3* and p-Chop, which could have contributed to the cytotoxicity of ZnO NPs. Moreover, *DDIT3*/p-Chop is also proinflammatory;[25,26] therefore, the induction of *DDIT3*/p-Chop might explain NP-induced inflammatory responses showing as increased sVCAM1 and sICAM1 release.

It is interesting to note that *KLF4* expression was significantly induced by TiO_2 NPs, as well as ZnO NPs to a much lesser extent. *KLF4* is a crucial transcription factor for SMC-phenotype switch.[11] In mice, SMC-specific conditional knockdown of *KLF4* reduced SMC-derived macrophage foam cells and thus increased the stability of atherosclerotic plaques.[27] Moreover, a recent study showed that induction of KLF4 mediated SMC reprogramming in vivo, which could potentially contribute to intimal lesions.[28] Therefore, it is expected that induction of *KLF4* in HASMCs might also lead to SMC-phenotype switch, although more work is needed to confirm this. However, it should also be noted that *CD68* expression remained unaltered after NP exposure. In diseased human blood vessels, SMCs express macrophage marker CD68 and thus contribute cholesterol accumulation in advanced atherosclerotic plaques.[29,30] The unaltered *CD68* expression indicated that TiO_2, ZnO, or Ag NP exposure might not promote SMC-derived macrophage formation.

Conclusion

Combined, the results from this study suggested that ZnO NPs, but not TiO_2 or Ag NPs at the same mass concentrations, were cytotoxic to HASMCs. We suggested that the cytotoxicity of ZnO NPs might be associated with increased intracellular Zn ions, ROS, and ER stress. Moreover, the induction of ER stress as increased *DDIT3* expression and p-Chop protein levels also mediated inflammatory responses. The expression of *KLF4* was modestly induced by ZnO NP exposure, which might have resulted in SMC-phenotype switch (Figure 7). However, the exact role of KLF4 activation in NP-induced toxic effects to SMCs might need further studies. Exposure to up to 64 μg/mL TiO_2 and Ag NPs did not induce cytotoxicity significantly, but might also promote the release of cytokines and promote the expression of *KLF4*. Therefore, it is possible that the toxicity of TiO_2, ZnO, and Ag NPs to HASMCs could be dependent on the composition of NPs. However, the conclusion of this study was primarily based on in vitro data, and the toxicity of metal-based NPs to SMC in vivo has to be confirmed in the future. Nevertheless, our results highlight the importance of investigating the toxic effects of metal-based NPs

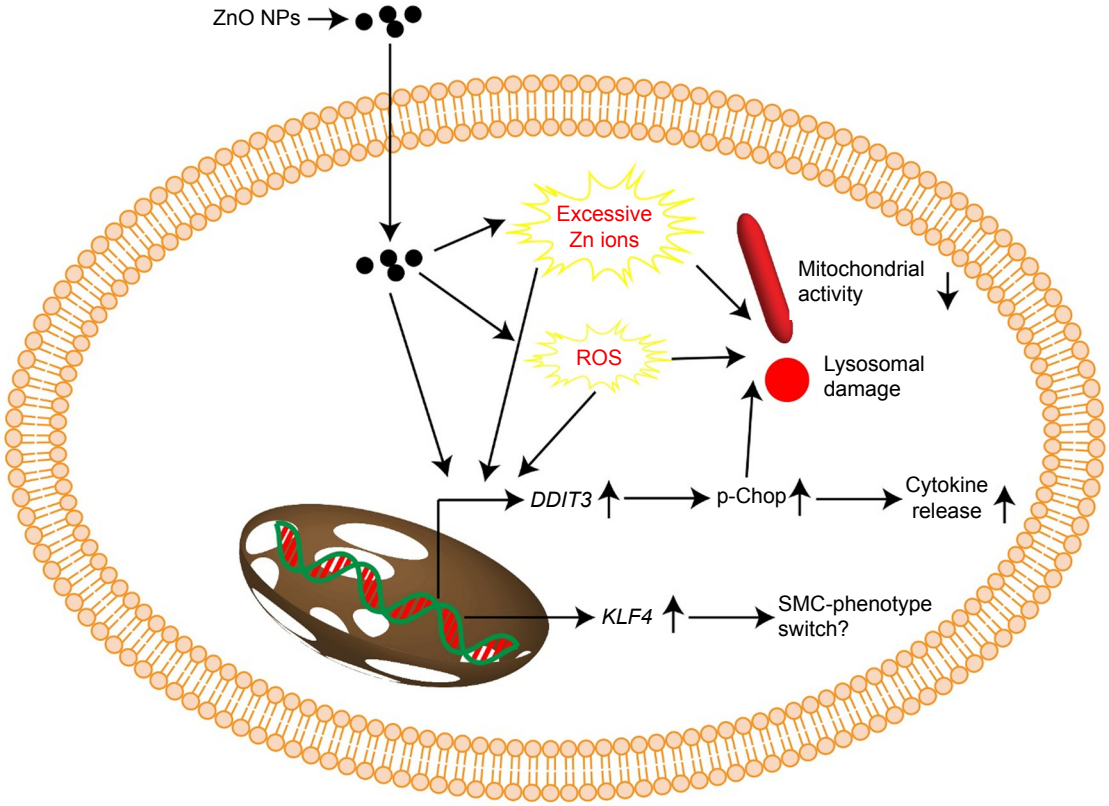

Figure 7 Proposed mechanism associated with toxicity of ZnO NPs to HASMCs.
Notes: Exposure to ZnO NPs might induce excessive Zn ions, ROS, and ER stress, leading to cytotoxicity. In addition, induction of KLF4 might also lead to SMC-phenotype switch.
Abbreviations: ER, endoplasmic reticulum; HASMCs, human aortic smooth-muscle cells; NPs, nanoparticles; ROS, reactive oxygen species.

to SMCs, in order better to understand the potential adverse vascular effects of NPs. From this perspective, we are also developing a coculture model based on alveolar cells and SMCs to investigate possible signaling communications between NP-exposed alveolar cells and SMCs.

Acknowledgments

This work was financially supported by the National Natural Science Foundation of China (grant 21707114) and Science and Technology Planning Program of Guangzhou City, People's Republic of China (201707010467).

Disclosure

The authors reports no conflicts of interest in this work.

References

1. Vance ME, Kuiken T, Vejerano EP, et al. Nanotechnology in the real world: redeveloping the nanomaterial consumer products inventory. *Beilstein J Nanotechnol*. 2015;6:1769–1780.
2. Cao Y, Gong Y, Liao W, et al. A review of cardiovascular toxicity of TiO_2, ZnO and Ag nanoparticles (NPs). *Biometals*. 2018;31(4):457–476.
3. Cao Y, Gong Y, Liu L, et al. The use of human umbilical vein endothelial cells (HUVECs) as an in vitro model to assess the toxicity of nanoparticles to endothelium: a review. *J Appl Toxicol*. 2017;37(12):1359–1369.
4. Setyawati MI, Tay CY, Docter D, Stauber RH, Leong DT. Understanding and exploiting nanoparticles' intimacy with the blood vessel and blood. *Chem Soc Rev*. 2015;44(22):8174–8199.
5. Lacolley P, Regnault V, Segers P, Laurent S. Vascular smooth muscle cells and arterial stiffening: relevance in development, aging, and disease. *Physiol Rev*. 2017;97(4):1555–1617.
6. Bennett MR, Sinha S, Owens GK. Vascular smooth muscle cells in atherosclerosis. *Circ Res*. 2016;118(4):692–702.
7. Minarchick VC, Stapleton PA, Fix NR, Leonard SS, Sabolsky EM, Nurkiewicz TR. Intravenous and gastric cerium dioxide nanoparticle exposure disrupts microvascular smooth muscle signaling. *Toxicol Sci*. 2015;144(1):77–89.
8. Cao Y, Long J, Ji Y, et al. Foam cell formation by particulate matter (PM) exposure: a review. *Inhal Toxicol*. 2016;28(13):583–590.
9. Liu J, Feng X, Wei L, Chen L, Song B, Shao L. The toxicology of ion-shedding zinc oxide nanoparticles. *Crit Rev Toxicol*. 2016;46(4):348–384.
10. Cao Y, Long J, Liu L, et al. A review of endoplasmic reticulum (ER) stress and nanoparticle (NP) exposure. *Life Sci*. 2017;186:33–42.
11. Fan Y, Lu H, Liang W, Hu W, Zhang J, Chen YE. Krüppel-like factors and vascular wall homeostasis. *J Mol Cell Biol*. 2017;9(5):352–363.
12. Long J, Xiao Y, Liu L, Cao Y. The adverse vascular effects of multi-walled carbon nanotubes (MWCNTs) to human vein endothelial cells (HUVECs) in vitro: role of length of MWCNTs. *J Nanobiotechnology*. 2017;15(1):80.
13. Cao Y, Jantzen K, Gouveia AC, et al. Automobile diesel exhaust particles induce lipid droplet formation in macrophages in vitro. *Environ Toxicol Pharmacol*. 2015;40(1):164–171.
14. Jiang Q, Li X, Cheng S, et al. Combined effects of low levels of palmitate on toxicity of ZnO nanoparticles to THP-1 macrophages. *Environ Toxicol Pharmacol*. 2016;48:103–109.

15. Danielsen PH, Cao Y, Roursgaard M, Møller P, Loft S. Endothelial cell activation, oxidative stress and inflammation induced by a panel of metal-based nanomaterials. *Nanotoxicology*. 2015;9(7):813–824.
16. Kermanizadeh A, Gosens I, Maccalman L, et al. A multilaboratory toxicological assessment of a panel of 10 engineered nanomaterials to human health – ENPRA project – the highlights, limitations, and current and future challenges. *J Toxicol Environ Health B Crit Rev*. 2016;19(1):1–28.
17. Gu Y, Cheng S, Chen G, et al. The effects of endoplasmic reticulum stress inducer thapsigargin on the toxicity of ZnO or TiO_2 nanoparticles to human endothelial cells. *Toxicol Mech Methods*. 2017;27(3):191–200.
18. Gong Y, Li X, Liao G, Ding Y, Li J, Cao Y. Cytotoxicity and ER stress–apoptosis gene expression in ZnO nanoparticle exposed THP-1 macrophages: influence of pre-incubation with BSA or palmitic acids complexed to BSA. *RSC Adv*. 2018;8(28):15380–15388.
19. Chang S, Zhao X, Li S, et al. Cytotoxicity, cytokine release and ER stress-autophagy gene expression in endothelial cells and alveolar-endothelial co-culture exposed to pristine and carboxylated multi-walled carbon nanotubes. *Ecotoxicol Environ Saf*. 2018;161:569–577.
20. Gonzalez C, Rosas-Hernandez H, Ramirez-Lee MA, Salazar-García S, Ali SF. Role of silver nanoparticles (AgNPs) on the cardiovascular system. *Arch Toxicol*. 2016;90(3):493–511.
21. Suzuki Y, Tada-Oikawa S, Ichihara G, et al. Zinc oxide nanoparticles induce migration and adhesion of monocytes to endothelial cells and accelerate foam cell formation. *Toxicol Appl Pharmacol*. 2014;278(1):16–25.
22. Gong Y, Ji Y, Liu F, Li J, Cao Y Cytotoxicity oxidative stress and inflammation induced by ZnO nanoparticles in endothelial cells: interaction with palmitate or lipopolysaccharide. *J Appl Toxicol*. 2017;37(8):895–901.
23. Chen R, Huo L, Shi X, et al. Endoplasmic reticulum stress induced by zinc oxide nanoparticles is an earlier biomarker for nanotoxicological evaluation. *ACS Nano*. 2014;8(3):2562–2574.
24. Logue SE, Cleary P, Saveljeva S, Samali A. New directions in ER stress-induced cell death. *Apoptosis*. 2013;18(5):537–546.
25. Zhang C, Syed TW, Liu R, Yu J. Role of endoplasmic reticulum stress, autophagy, and inflammation in cardiovascular disease. *Front Cardiovasc Med*. 2017;4:29.
26. Ghemrawi R, Battaglia-Hsu SF, Arnold C. Endoplasmic reticulum stress in metabolic disorders. *Cells*. 2018;7(6):E63.
27. Shankman LS, Gomez D, Cherepanova OA, et al. KLF4-dependent phenotypic modulation of smooth muscle cells has a key role in atherosclerotic plaque pathogenesis. *Nat Med*. 2015;21(6):628–637.
28. Majesky MW, Horita H, Ostriker A, et al. Differentiated smooth muscle cells generate a subpopulation of resident vascular progenitor cells in the adventitia regulated by Klf4. *Circ Res*. 2017;120(2):296–311.
29. Vengrenyuk Y, Nishi H, Long X, et al. Cholesterol loading reprograms the microRNA-143/145-myocardin axis to convert aortic smooth muscle cells to a dysfunctional macrophage-like phenotype. *Arterioscler Thromb Vasc Biol*. 2015;35(3):535–546.
30. Allahverdian S, Chehroudi AC, Mcmanus BM, Abraham T, Francis GA. Contribution of intimal smooth muscle cells to cholesterol accumulation and macrophage-like cells in human atherosclerosis. *Circulation*. 2014;129(15):1551–1559.

Supplementary materials

Table S1 Forward (F) and reverse (R) primers used in this study

Gene	ID	F-primer	R-primer	Product length
GAPDH	2,597	ACAGCCTCAAGATCATCAGC	GGTCATGAGTCCTTCCACGAT	104 bp
DDIT3	1,649	GGAAACAGAGTGGTCATTCCC	GGAAACAGAGTGGTCATTCCC	116 bp
XBP1S	7,494	CCGCAGCAGGTGCAGG	GAGTCAATACCGCCAGAATCCA	70 bp
ATF6	22,926	AACTTTCCGTGACTAAACCTG	CCTTTAATCTCGCCTCTAACCC	165 bp
ERN1	2081	GCCTCCAACCACTCGCTCT	TCAAACATGCCCCGGTACACA	182 bp
KLF4	9,314	AAGTCCCGCCGCTCCATTACCAA	CATCATCCCGTGTGTCCCGAAG	101 bp
CD68	968	CCCACCTGCTTCTCTCATTCCC	TACTCCACCGCCATGTAGCTC	100 bp

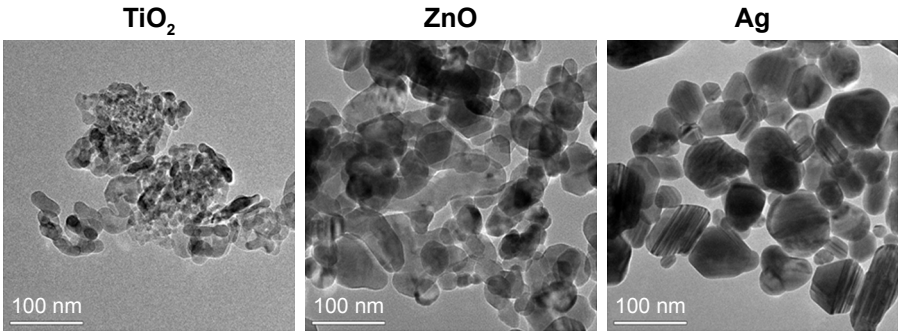

Figure S1 Transmission electron microscopy morphology of TiO_2, ZnO, and Ag nanoparticles.

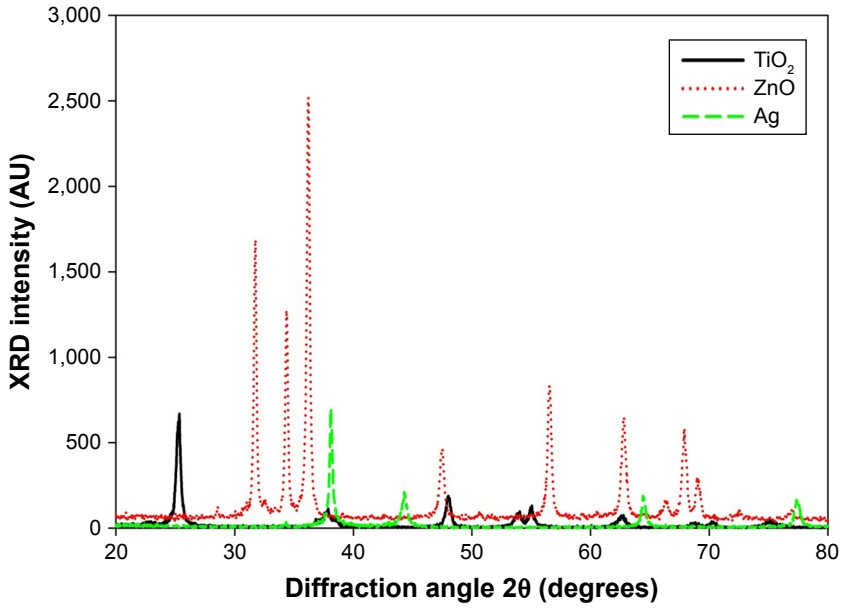

Figure S2 X-ray diffraction (XRD) spectra of TiO_2, ZnO, and Ag nanoparticles.

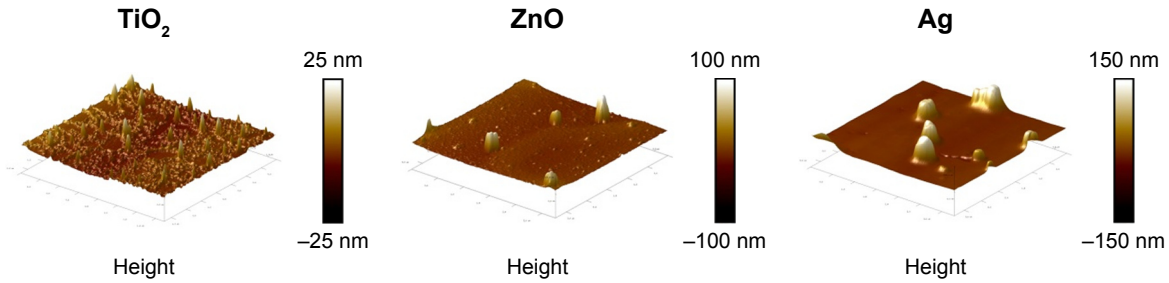

Figure S3 Topography of TiO_2 (left), ZnO (middle), and Ag nanoparticles (right) investigated by atomic-force microscopy.

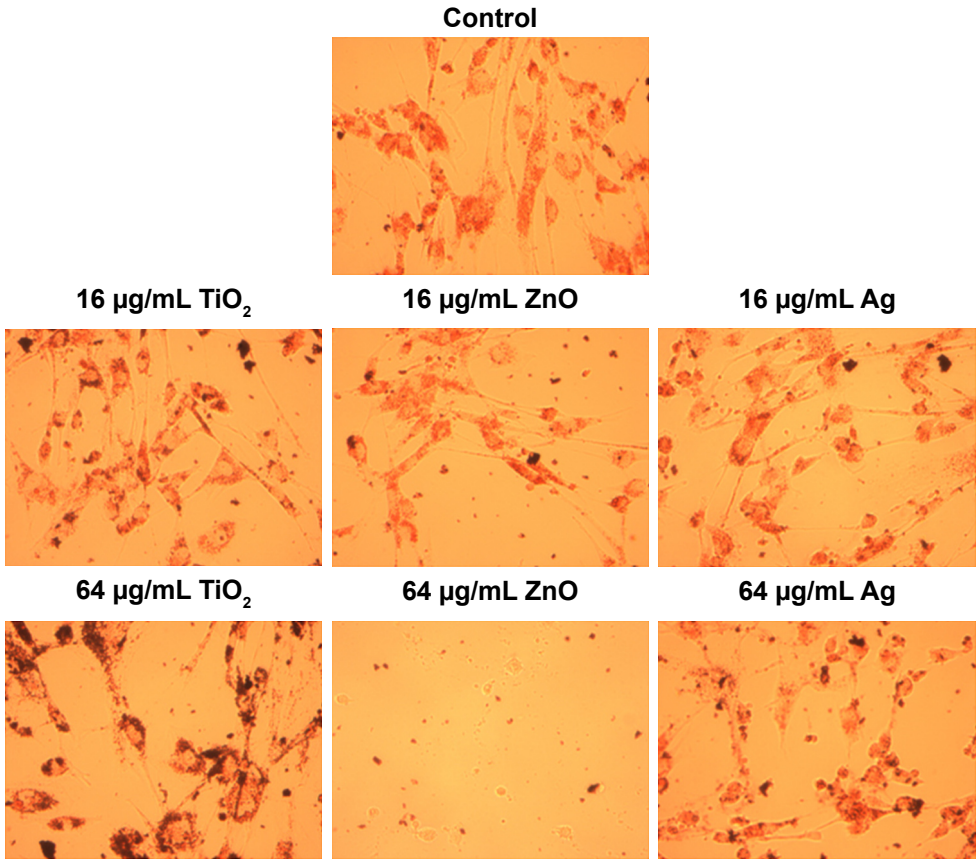

Figure S4 Representative images showing neutral red staining of HASMCs after NP exposure.
Notes: HASMCs were exposed to 0 µg/mL (control), 16 µg/mL, and 64 µg/mL TiO_2, ZnO, or Ag NPs for 24 hours, and then stained with neutral red. Images taken under light microscopy (magnification 200×).
Abbreviations: HASMCs, human aortic smooth-muscle cells; NPs, nanoparticles.

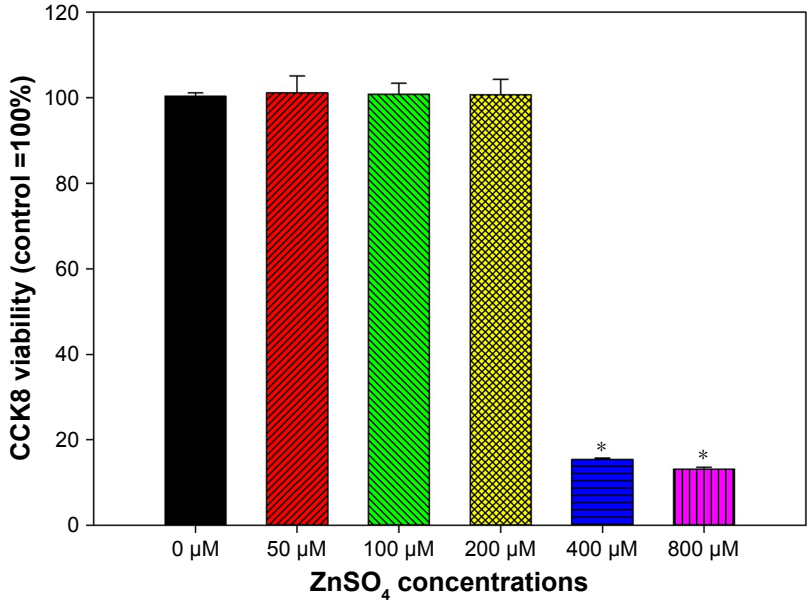

Figure S5 Cytotoxicity of $ZnSO_4$ on human aortic smooth-muscle cells.
Notes: Cells were exposed to various concentrations of $ZnSO_4$ for 24 hours and CCK8 assays were done to indicate cytotoxicity. *$P<0.01$ compared to control.
Abbreviation: CCK8, cell counting kit-8.

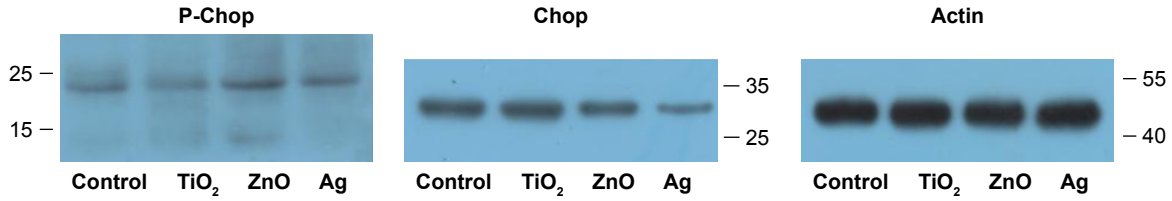

Figure S6 Unedited Western blot images.